REFINEMENT STRENGTHENING OF A NOVEL LOW COST-HIGH PROPERTIES AUSTENITIC STAINLESS STEEL VIATWIP/TRIP EFFECTS *

Renbo Song [1]
Yang Su [2]
Hengjun Cai [3]
Jian Wen [4]
Tianyi Wang [5]
Ke Guo [6]

Abstract

Controlling the phase reversion annealing process is commonly applied to deep cold-worked metastable austenitic to produce austenitic stainless steel with different types of austenite grain size from ultrafine grain to coarse grain and eliminating the work hardening. In this study, a novel low-cost Cr-Mn austenitic stainless steel (20LH5) is employed. After the phase reversion process, microstructures were observed by X-ray diffraction (XRD) and transmission electron microscopy (TEM). The results showed that annealing at 900 ℃+30 s can minimize the grain size to fine grain (FG: ~1 μm), which performed significant improvements in the mechanical properties with tensile strength ~1080 MPa, yield strength ~530 MPa and elongation rate ~47%, while annealing at 1100 ℃+30 s of the counterpart samples, the tensile strength is ~910 MPa, the yield strength is ~360 MPa and elongation rate is about 30% in the coarse grain (CG: ~7 μm) stainless steel. The deformation mechanism of the FG mainly contributes to the TWIP effects while in CG the deformation mechanism mainly relies on the TRIP effects.

Keywords: Phase reversion; 20LH5 stainless steel; Deformation mechanism.

[1] *Ph.D., School of Materials Science and Engineering, University of Science and Technology Beijing, Beijing, China.*

[2] *M.S., School of Materials Science and Engineering, University of Science and Technology Beijing, Beijing, China.*

[3] *Ph.D., Lianzhong (Guangzhou) Stainless Steel Corporation, Guangzhou, Guangdong, China.*

[4] *B.S., Lianzhong (Guangzhou) Stainless Steel Corporation, Guangzhou, Guangdong, China.*

[5] *M.S., School of Materials Science and Engineering, University of Science and Technology Beijing, Beijing, China.*

[6] *Ph.D., School of Chemical Engineering, University of Science and Technology Liaoning, Angang Group Mining Design and Research Institute Co., Ltd, Anshan, Liaoning, China.*

1 INTRODUCTION

Austenitic stainless steel is commonly used in applications where corrosion resistance is highly required[1]. The expensive Ni is contributing to the corrosion resistance and the result that the overall cost of the steel stays high. According to the metallography, in order to stabilize the austenitic stainless steel the C, N and Mn can be implemented in lieu of Ni to compromise between the properties and cost [2]. Besides, improving the strain hardening behavior and mechanical properties by adding nitrogen will make sense, metastable austenitic stainless steel is an important kind of austenitic stainless steel in which γ-austenite will transform to *α'*-martensite during deformation, thus metastable austenitic stainless steel will present a better tensile strength and formability than stable ones, the metastable austenitic stainless steel is serving in railway and automobile structure components due to the safety and weight reduction[3]. However, it is worthy of mentioning that the low yield strength limits the horizon of the application. Some methods such as solution hardening, precipitation hardening, and grain refinement can improve the yield strength. Grain refinement is an effective way to increase the yield strength without impairing the ductility.

In order to gain the strength and ductility at the same time, large quantity of researches have focused on the nano/ultra-fine grain austenitic and some measures such as high-pressure torsion, equal-channel angular pressing and accumulative roll bonding [4] proved to be successful. Furthermore, advanced thermodynamics method is another effective way including cold rolling and annealing, in general, the second method is more suitable for actual practice [5].

We formerly researched the effect of deformation on strain hardening behavior and the strength-ductility combination of a novel 20LH5 stainless steel with a conventional grain size of 1 μm with both TRIP (transformation induced plasticity) and TWIP effects (twinning induced plasticity). Challa et al. have invested the influence of phase reversion on grain size and mechanical properties. In this passage, we discussed a comparison of mechanical properties of phase reversion 20LH5 stainless steel with that of coarse-grained counterpart to give evidence of the grain refinement advantages.

2 EXPERIMENT PROCEDURES

2.1 Test materials

The experimental materials were the novel 20LH5 low-Ni Cr-Mn austenitic stainless steel with the composition listed in Table 1. The inner structures are austenitic with grain size ~1μm to ~10μm as measured according to the liner-intercept method (ASTM E122).

2.2 Phase reversion annealing

The plates were first cold rolled in a laboratory rolling mill to 63% reduction in thickness (0.55 mm). The plate was then annealed for stress relief and subsequently cold rolled to 0.3 mm before annealing for solution treatment. The annealing temperature for stress relief was varied in the range of 350-450 ℃ and the holding time varied between 10 and 120s. The change in annealing temperature-time sequence allowed us to find the best stress relief state by comparing the elongation rate and yield ratio. Following cold rolling, all samples were annealed with the temperature range from 900-1100 ℃ and holding time varied between 5 and 15 s for solution treatment then cooled in water to ensure the cooling rate above 200 ℃/s , the change in annealing temperature-time sequence enabled us to obtain a wide range of grain size from mix grain (MG), fine grain (FG) to coarse grain (CG) regime. The annealing conditions were so selected that there was a complete reversion of martensite to austenite. The process graph is showed in Fig. 1

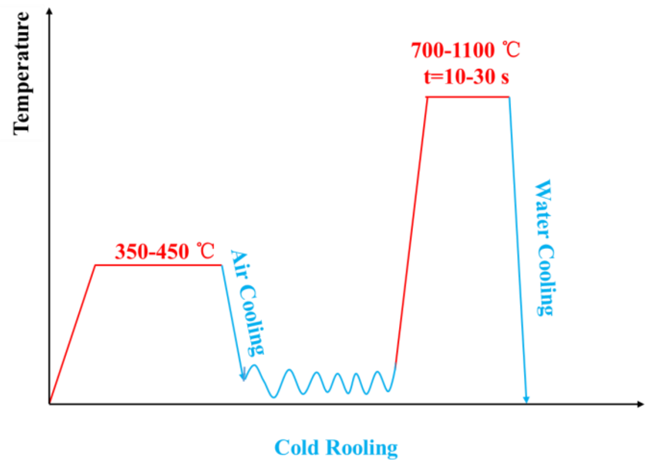

Fig.1. Process graph of the novel 20LH5 stainless steel plate

Table1 Chemical composition of 20LH5 austenitic stainless steel in wt%

C	Si	Mn	Ni	Cr	Cu	N
0.08	0.52	10.35	0.62	14.04	0.88	0.18

2.3 Microstructural characterization

Tensile tests were conducted by machining phase reversion annealed A_{50} nonstandard specimens, the shape and size are showed in Fig. 2. The mechanical properties were measured at a constant rate 0.05 s^{-1} with the tensile machine CMT 4105 tensile machine, furthermore, three nonstandard samples were cut in the rolling direction and tested for each condition.

Microstructures were observed by an optical microscope (OM). To study the deformed microstructure as a function of strain, area with the highly stressed region through the plate length was used for preparation of transmission electron microscope (TEM) foils which were prepared by twin-jet electropolishing of 3 mm with the electrolyte solution of 7% perchloric acid-acetic acid from a number of tensile-tested specimens for ε=0.02, 0.1, 0.2.

The volume fractions of strain-induced martensite were averaged through the X-ray diffraction (XRD) analysis.

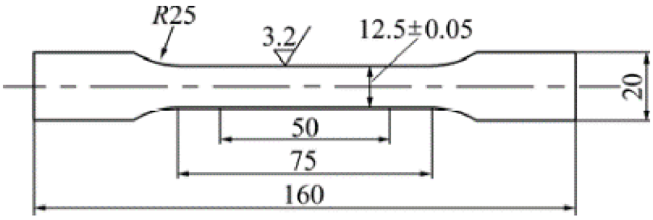

Fig. 2. Shape and size of A50 nonstandard specimen(mm).

3 RESULTS and DISSCUSSION

3.1 Mechanical properties

The results of the uniaxial tensile tests conducted among the mix grain (MG), fine grain (FG) and coarse grain (CG) are shown in Fig.3, the ductility of MG structure is the worst: tensile strength ~1345 MPa, yield strength ~1233 MPa, and elongation rate ~7.72%, while the CG structure performed better with tensile strength ~972 MPa, yield strength ~422 MPa, and elongation rate ~34.86%, furthermore, the FG structure shows the best with tensile strength ~1082 MPa, yield strength ~530 MPa, and elongation rate 47.66%. Two main kinds of deformation mechanism are activated in the deformation process, that is, the strain-induced martensite (the TRIP effect) and mechanical twining (the TWIP effect), the annealing process plays a deceive role in influencing the mechanical properties.

In Fig 3, it can be seen that the yield and tensile strength is increasing below 900 ℃, than dropping down in over 900°C, for instance, the yield strength is 600MPa and tensile strength is 1100MPa, which are obtained in annealing at 900 ℃ + 30 s with the grain size of 1.5 μm. Then, the fracture elongation is high, about 45%. Hence, the yield strength is almost doubled by the reversion treatment compared to that of the conventional steel with the grain size of 15–18 μm. A further advantage is that the anisotropy in mechanical properties, present in work-hardened grades, disappears in annealing [6]. As observed in the present study, the yield stress is strongly influenced by the grain size and significant improvement could be achieved by the grain size by refinement from 10–20 μm to 1–2 μm during reversion treatment, and the strengthening mechanisms have been discussed in detail in previous papers[7].

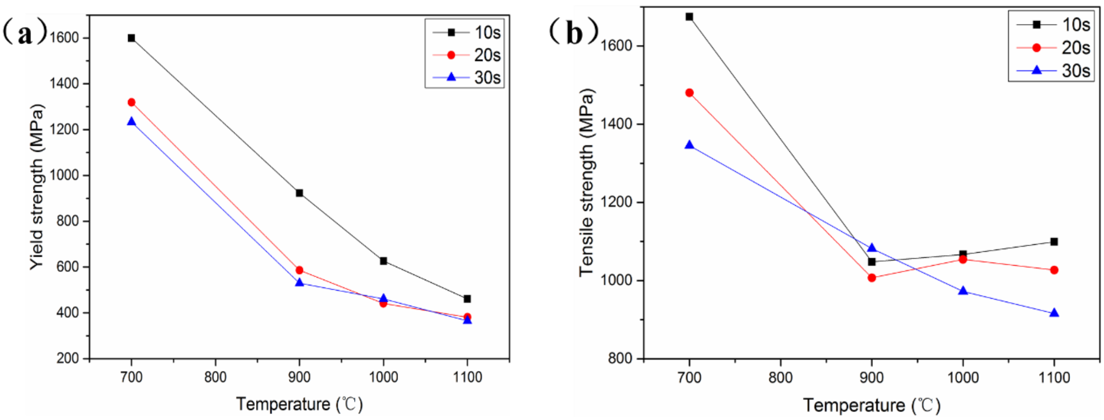

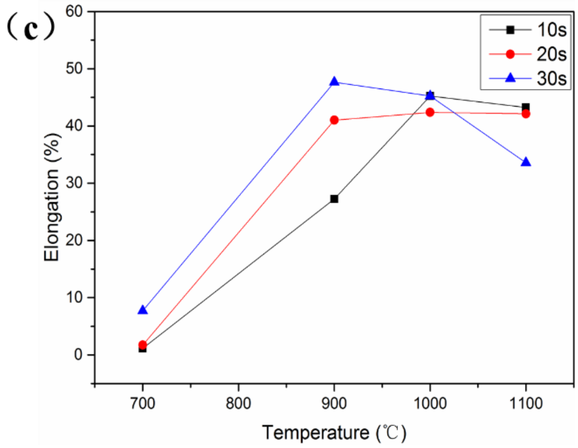

Fig. 3. Mechanical properties of 20LH5 after phase reversion in different temperature – time annealing, (a) yield strength (b) tensile strength (c) elongation rate.

XRD patterns of the MG, FG and CG in different strain of 0.02, 0.1, 0.2 is plotted (Fig. 4), it is seen that at lower strain of 0.02, straining induced the lowest degree of martensite transformation in FG while the CG is the highest, then gradually increase with the strain increase to 20%, by analyzing the graph, it can be calculated that in FG of ε=0.02 (Fig. 4(a)), there are very small amount of the α`-martensite (≈3%) and most of which is γ (≈70%), in ε=0.1 (Fig. 4(b)), the α`-martensite (≈4%) increased ~1% and γ (≈40%) decreased sharply ~30%, while in ε=0.2 (Fig. 4(c)), small increase can be seen in α`-martensite (≈6%) and γ dropped significantly to ~10%, the same trend of revolution of γ can be seen in both CG and MG. however, the graph also indicted that the CG structure is much more sensitive to the deformation and in ε=0.02 the martensite increase dramatically to ~96% compared to the MG ~40% and FG ~3%, which is the typical TRIP effects during the deformation process.

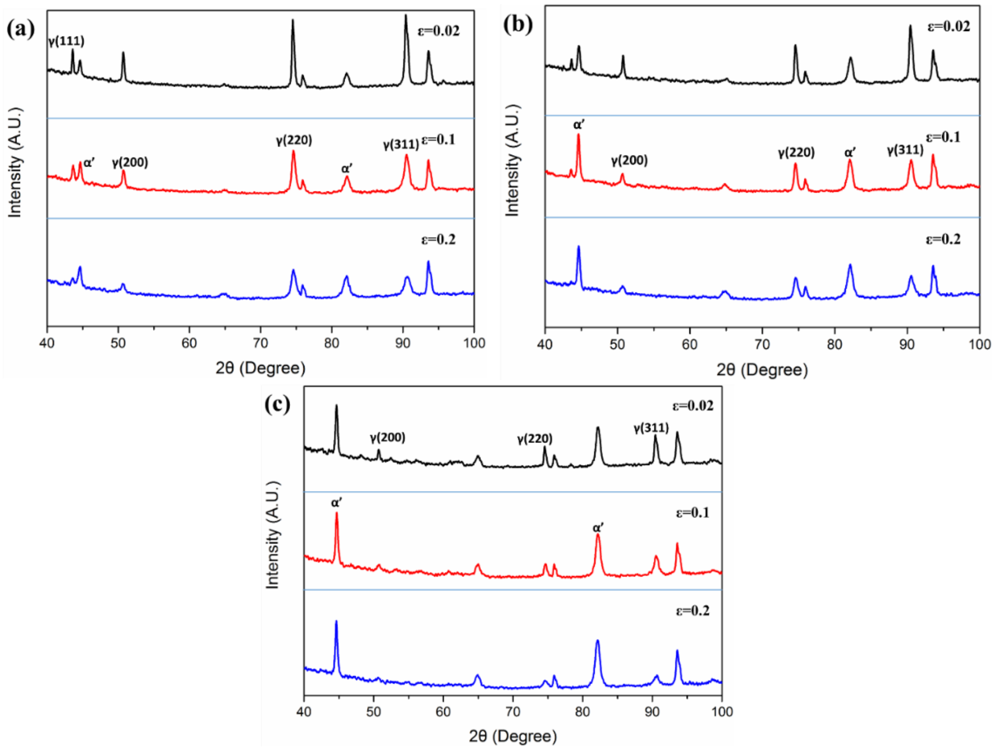

Fig.4. XRD patterns of the different grain size at different strain (ε=0.02, 0.1, 0.2) (a) MG (b) FG (c) CG.

3.2 Microstructures analyses

With 80% cold rolling reduction of the whole process, the majority of the cold-rolled microstructure is the α`-martensite[8], in phase reversion temperature range from 700 ℃ to 1100 ℃, the strain induced martensite tends to revert back to austenite with fine grain size by diffusional or shear reversion mechanism[9]. Furthermore, the grain refinement of the deformed retained austenite grains require the occurrence of static recrystallization, which need relatively higher temperatures and long-term annealing indeed.[10]

Large quantity of researches have proved that with the increasing reduction in thickness, the density of dislocation and slip bands will increase significantly. Thus, the structure of the cold-rolled grain structure is hindered and cannot be found by EBSD.[11] Fig. 5 showed the evolution process of the phase reversion in microstructure vary in temperatures. In Fig 5(a), the microstructure of 700 ℃+30 s shows that there are plenty of mixture grains with the grain size from ~1 μm (reverted grains) to ~20 μm (retained grains). Grain refinement will occur in higher temperature with the same annealing time of 30 s in 900℃, where the average grain size is ~1 μm, grains are formed by activating the static recrystallization (showed in Fig. 5(b)), the grain size tend to spread homogenize. Fig. i5(c) unveil the microstructure of the grain annealed in 1100 ℃+30 s, the grain size is coarse with ~7 μm.

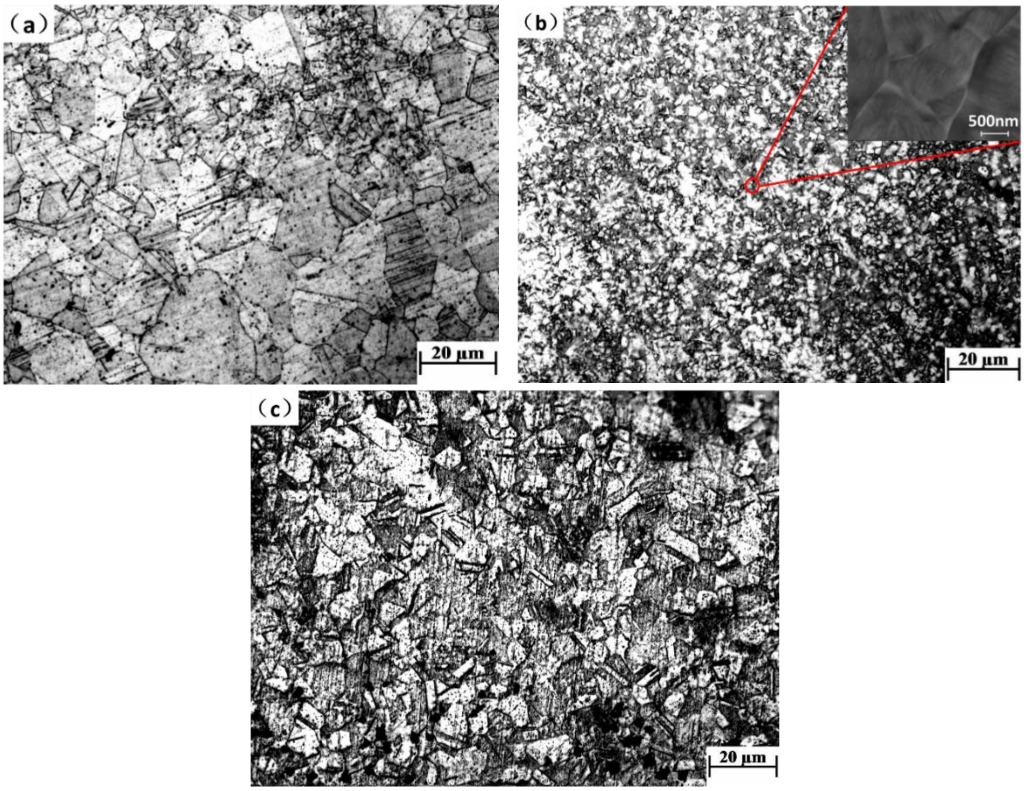

Fig. 5. Phase reversion of annealed microstructure of time-temperature (a) 700℃+30s (b) 900℃ +30s (c) 1100℃+30s.

3.3 Discussion

By using TEM after straining to certain strain, the microstructural evolution as a function of selected strain for different grain size is presented in Fig. 6-7. In the FG structure (shown in Fig. 6(a)), there are quantities of stacking faults at low strain (ε=0.02) due to the movement of a/6<112> Shockley partial dislocations on the close-packed {111} planes of austenite [12]. The microstructure in Fig. 6(b) reveals that twins grow in different directions and mutually intersect one another, which are arranged in primary and conjugate slip systems. This indicated that a low SFE close packed alloy and meets the theory of multiple slips at the oncoming of deformation. At appreciably higher strain of ε=0.2 (Fig.6(c)), the density of twins can be observed and organized in bundles, the diffraction pattern confirmed the presence of deformation twins. Furthermore, the dark areas which can be seen in Fig. 6(d) are presumably α`-martensite with quantities of micro shear bands.

Fig.7 summarizes the representative TEM micrographs of the deformation processes associated with the tensile straining for the CG structure, a large number of dislocations and martensite in straight and thin state were observed (Fig.7(a)), when the strain increased to 0.1, a large number of lathlike martensite nucleated at shear bands and grow in one direction (Fig. 7(b)), with the increase in strain to 0.2, the martensite laths became thicker (Fig. 7(c), (d)), the thickness of the lath increase from 1 μm to 1.8 μm when the strain increase from 0.1 to 0.2.

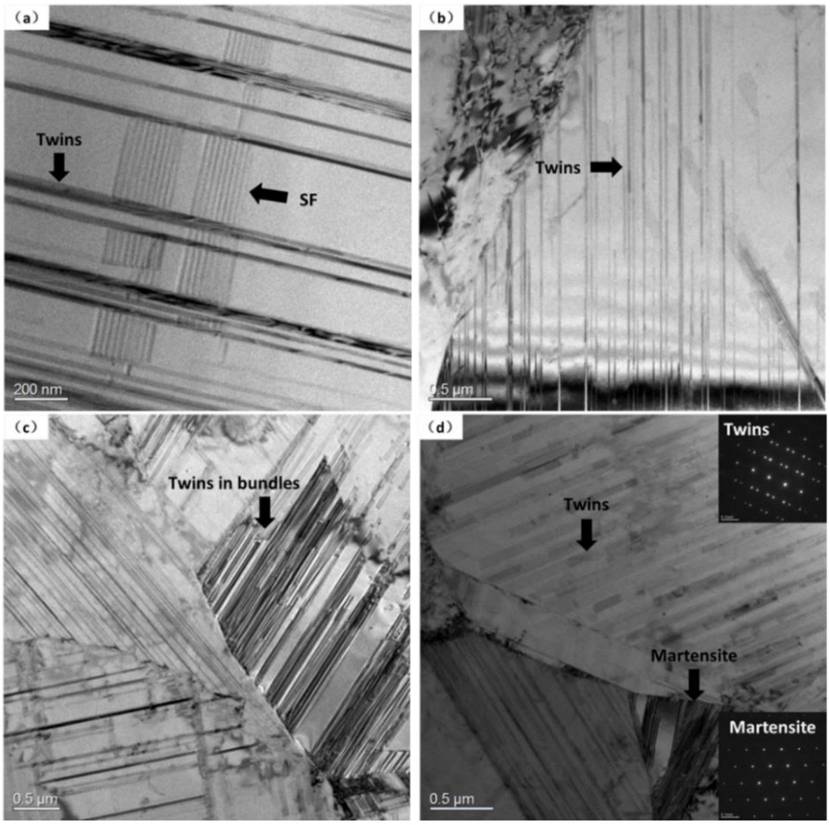

Fig. 6. Representative bright field transmission electron micrographs of FG structure at (a) ε=0.02, (b) ε=0.1, (c) twins in ε=0.2 (d) α`-martensite in ε=0.2.

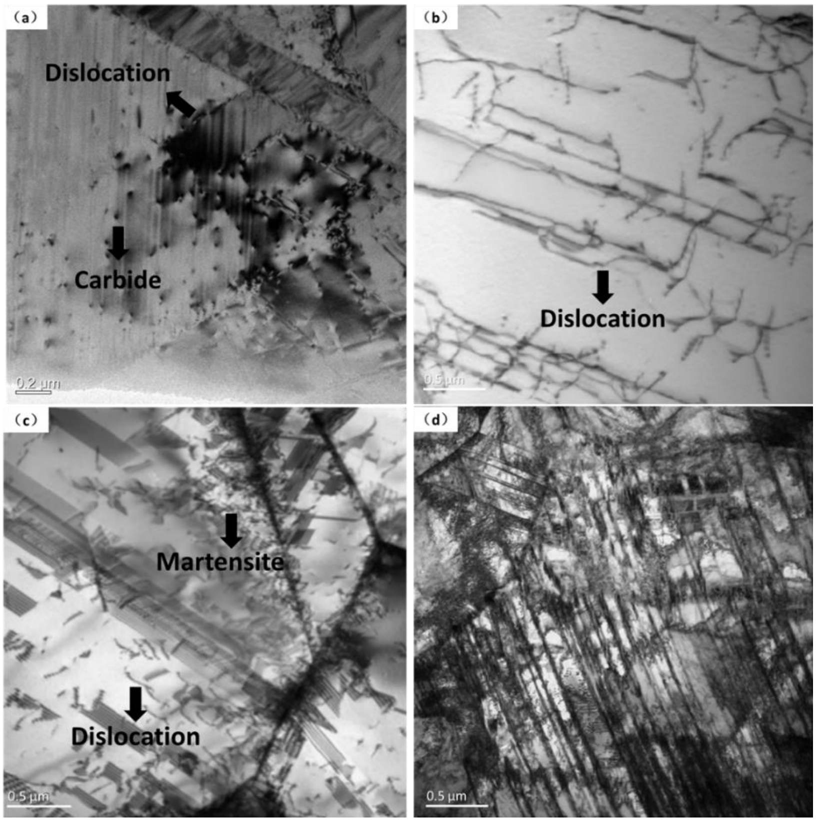

Fig. 7. Representative bright field transmission electron micrographs of CG structure (a) ε=0.02, (b) ε=0.1, (c) thin lathlike martensite in ε=0.2 (d) thick lathlike martensite in ε=0.2.

In general, the solubility of C in high-temperature ferrochrome-nickel austenite (iron-based) is relatively large, and the carbon content in common chrome-nickel austenite stainless steel can reach 0.15% (quality percentage). Austenitic stainless steel dissolved in C at high temperatures is rapidly cooled to room temperature and C is dissolved in a supersaturated form.[13] however, if reheated to the right temperature and kept for enough time, the supersaturated C will precipitate out in the form of carbides, resulting in poor chromium near the grain boundary of stainless steel. In austenitic stainless steel without Ti, Nb and other strong carbide forming elements, $Cr_{23}C_6$ is the most important carbide, and its precipitation temperature ranges from 400℃ to 800℃. Precipitation kinetics depends on the chemical composition of the steel and previous processing, with carbon having the greatest impact. The decrease of carbon content delayed the precipitation time of $Cr_{23}C_6$ and shifted the temperature range of carbides to the low temperature.

Considering the effect of precipitates on mechanical properties, the carbon content of commonly used austenitic stainless steel is less than 0.15% (mass percentage), so the precipitation temperature of carbide is lower than 800℃. At the heat treatment temperature of 700℃, there were obvious precipitates on the grain boundary of MG (Fig. 8 (a)), while at the heat treatment temperature of 900℃ (Fig. 8 (b)), there were no precipitates on the grain boundary of FG tissues, never the less, some carbide precipitate was detected in CG structure(Fig. 8 (c)) due to the over high temperature, which have bad effect on the mechanical properties.

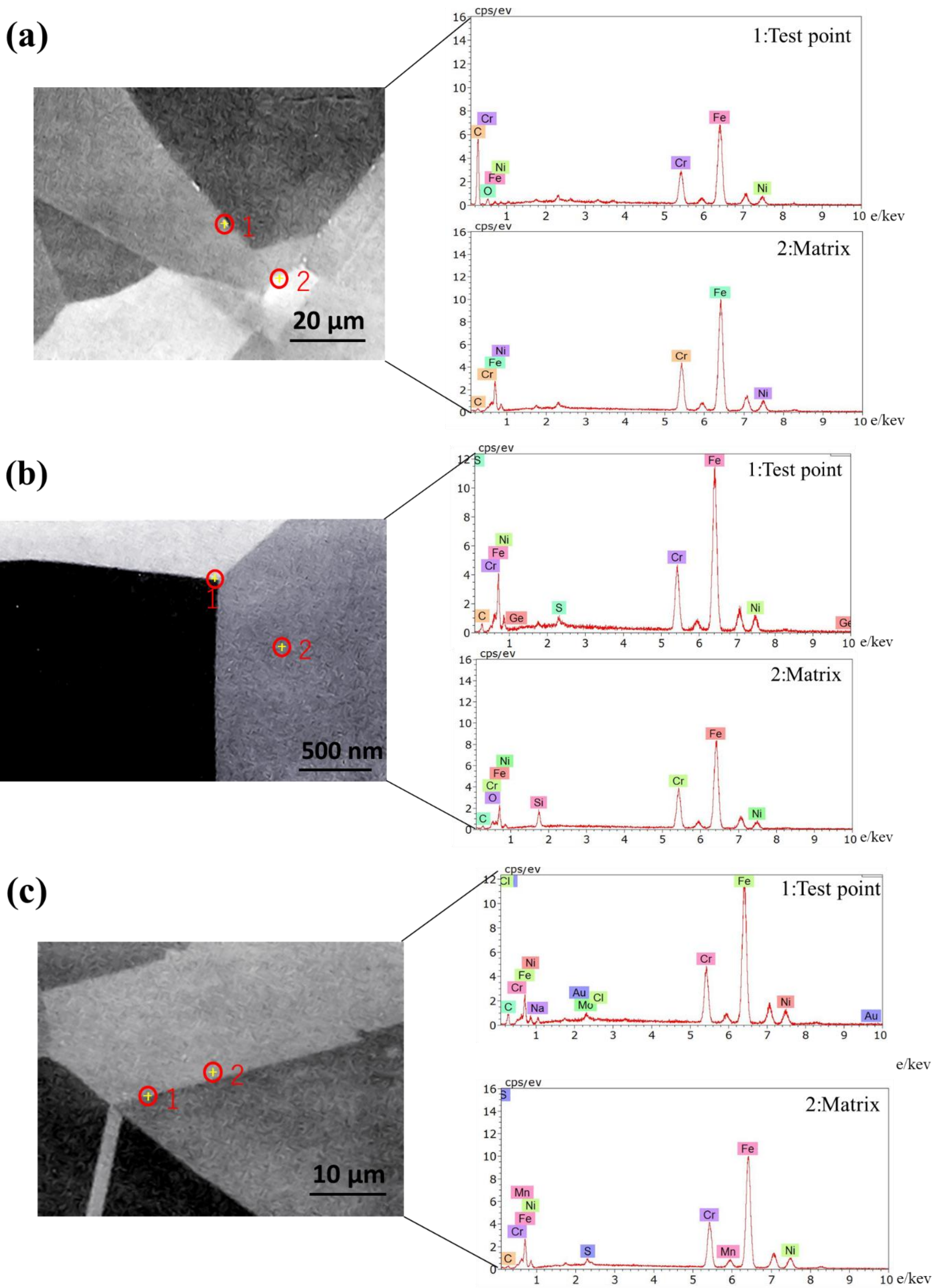

Fig 8. Precipitation of carbide behavior (a)MG (b)FG (c)CG.

4 RESULTS

The concept of phase reversion is applied in the novel 20LH5 stainless steel to obtain the plate of MG, FG and CG structures, we have elucidated here the interplay from FG to CG both in mechanical properties and microstructures and can be summarized as follows:

(1) Heavy load cold rolled and annealing is an effective way to refine the grain size reverse form austenite to martensite, the grain refinement improves its mechanical properties either in strength (tensile and yield) or elongation remarkably, which makes it superior than the conventional cold work-hardened or the heat treatment stainless steel.

(2) the deformation mechanism of the FG mainly contributes to the TWIP effects while in CG the deformation mechanism mainly relies on the TRIP effects, however the MG structure stainless steel perform the worst caused by the uneven structure and carbide precipitation during deformation but not TWIP+TRIP effects.

5 REFERENCE

[1] Liu, Wei. "SA213-TP304Austenitic Stainless Steel Solid Solution Treatment Technology and Application." Mechanical Management & Development (2014).

[2] Ge, Dafang, et al. "Comparison of Two Typical Heat Treatment Process for ZG15CrMo Steel." Heat Treatment of Metals (1998).

[3] Robinson, S. L., et al. "Strain-aging in highly worked 316L stainless steel." Practical Failure Analysis 1.2(2001):83-92.

[4] Moor, E. De, et al. "Effect of Retained Austenite Stabilized via, Quench and Partitioning on the Strain Hardening of Martensitic Steels." Metallurgical & Materials Transactions A 39.11(2008):2586.

[5] Mészáros, István, and J. Prohászka. "Magnetic investigation of the effect of α′-martensite on the properties of austenitic stainless steel." Journal of Materials Processing Tech 161.1(2005):162-168.

[6] Juntunen, Pasi, et al. "Optimizing continuous annealing of interstitial-free steels for improving deep drawability." Metallurgical & Materials Transactions A 32.8(2001):1989-1995.

[7] Fenili, Cleber Pereira, et al. "Effect of sensitization on tribological behavior of AISI 304 austenitic stainless steel." International Journal of Materials Research 109.3 (2018): 234-240.

[8] Mahajan, S. "Critique of mechanisms of formation of deformation, annealing and growth twins: Face-centered cubic metals and alloys." Scripta Materialia 68.2 (2013): 95-99.

[9] Tsakiris V, Edmonds D V. Martensite and deformation twinning in austenitic steels[J]. Materials Science and Engineering: A, 1999, 273: 430-436.

[10] Lee T H, Shin E, Oh C S, et al. Correlation between stacking fault energy and deformation microstructure in high-interstitial-alloyed austenitic steels[J]. Acta Materialia, 2010, 58(8): 3173-3186.

[11] Takaki S, Fukunaga K, Syarif J, et al. Effect of grain refinement on thermal stability of metastable austenitic steel[J]. Materials Transactions, 2004, 45(7): 2245-2251.

[12] Karjalainen L P, Taulavuori T, Sellman M, et al. Some strengthening methods for austenitic stainless steels[J]. steel research international, 2008, 79(6): 404-412.
[13] Akbari A, Mohammadzadeh R. Effect of Grain Refinement on the Mechanical Properties of a Nickel- and Manganese-Free High Nitrogen Austenitic Stainless Steel[J]. Metallurgical and Materials Transactions A, 2015, 46(4):1570-1579.